The Total Hemispheric Emissivity of Painted Aluminum Honeycomb at Cryogenic Temperatures

J. Tuttle, E. Canavan, M. DiPirro, X. Li, and P. Knollenberg[1]

NASA Goddard Space Flight Center, Code 552
Greenbelt, Maryland, 20771, USA

[1]Northrop Grumman Aerospace Systems
Redondo Beach, CA 90278, USA

ABSTRACT

NASA uses high-emissivity surfaces on deep-space radiators or thermal radiation absorbers in test chambers. Aluminum honeycomb core material, when coated with a high-emissivity paint, provides a lightweight, mechanically robust, and relatively inexpensive black surface that retains its high emissivity down to low temperatures. At temperatures below about 100 Kelvin, this material performs much better than the paint itself. We measured the total hemispheric emissivity of various painted honeycomb configurations using an adaptation of an innovative technique developed for characterizing thin black coatings. These measurements were performed from room temperature down to 30 Kelvin. We describe the measurement technique and compare the results with predictions from a detailed thermal model of each honeycomb configuration.

KEYWORDS: emissivity, total hemispheric emissivity, painted aluminum honeycomb, space flight radiators.

INTRODUCTION

High emissivity (black) surfaces are often used on radiators flying on NASA missions. The radiators emit heat to deep space, cooling science instruments down to their cryogenic operating temperatures. The power radiated from a surface is described by the Stefan-Boltzmann Equation,

$$\dot{Q} = \sigma A \varepsilon T^4, \tag{1}$$

where $\dot{Q}$ is the total radiated power in Watts, T is the surface temperature in Kelvin, A is the surface area in m^2, $\sigma = 5.67 \times 10^{-8}$ Watts/m^2/K^4 is the Stefan-Boltzmann constant, and ε is the surface's total hemispheric emissivity. It is important for the radiating surface to be very black, with an ε value close to 1.0. NASA also employs such surfaces on thermal absorbers in large cryogenic test chambers. In this application the cold, black surface simulates the deep space environment, allowing engineers to test their thermal models. To achieve this high emissivity at cryogenic temperatures in a mechanically robust coating over a large area, there are few options. Many black paints have been shown to withstand the rigors of cryogenic temperatures and space flight, but their emissivities all drop to significantly lower values below about 100 Kelvin. Ball Infrared Black™ (BIRB™) remains very black down to low temperatures [1], but it is a proprietary coating produced only by Ball Aerospace and Technologies, Corp. For other organizations desiring a large black surface at cryogenic temperatures, painted aluminum honeycomb core is relatively cheap, lightweight, and effective.

The James Webb Space Telescope (JWST) will include several radiators operating at about 35 Kelvin, and their ability to emit the maximum possible heat to deep space is critical to the mission success. For some of these radiators painted aluminum honeycomb was chosen to provide the black surfaces. In the interest of reducing spacecraft mass, the goal was to find a lightweight honeycomb configuration which still produced a very high effective surface emissivity in the operating temperature range. We had developed a practical method of measuring the total hemispheric emissivity of low temperature thin coatings and had used it to characterize BIRB™ [1]. We modified this method to allow similar measurements on painted honeycomb core samples, and we characterized three different honeycomb configurations with successively decreasing mass per unit area.

THEORY

Painted honeycomb has a high total hemispheric emissivity due to its convoluted geometry. For radiators, the cell walls provide a large effective emitting area. On absorbers, the incoming radiation reflects multiple times off the walls, enhancing the absorptance. Aluminum alloys are typically selected for the cell walls due to their relatively high thermal conductivities. The honeycomb product can be purchased as open-cell core material, and it is painted before bonding one side to a heat-sink plate (also usually aluminum). The un-bonded open ends of the cells provide the emitting or absorbing surface.

In 1964 Sparrow et al. calculated the effective emissivity of cylindrical holes [2]. The authors showed that three characteristics of a hole increase its emissivity: a large aspect ration (depth/radius), high surface emissivity on the hole wall, and wall surfaces for which most radiation which reflects does so specularly. Here specularity is defined as the fraction of radiation reflecting from a surface as it would from a mirror, with no scattering. For very low-aspect-ratio holes the emissivity increases with larger aspect ratio. However, for totally diffuse reflections (zero % specular) and a given wall emissivity, the hole's emissivity remains constant for aspect ratios larger than some critical value. For very specular reflections the hole's emissivity continues to rise, asymptotically approaching a value of 1.0, as the aspect ratio increases.

We constructed a Thermal Desktop™ model of a hole and varied its aspect ratio, surface emissivity, and specularity to confirm that we duplicated Sparrow's results. Then we built a similar model of a hexagonal hole in order to predict the performance of honeycomb samples. FIGURE 1 shows the predicted behavior of a hexagonal hole with
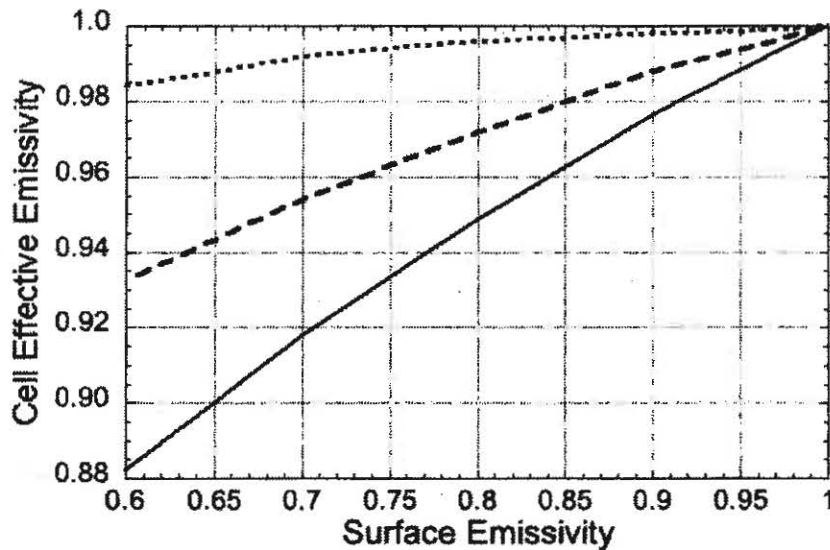
FIGURE 1. The calculated effective emissivity of a hexagonal hole with R/L = 6. The solid, dashed and dotted lines represent fully diffuse, 50% specular, and fully specular reflections off the walls.

aspect ratio of 6 and surface emissivity of greater than 0.6, which match the characteristics of two of our test samples. The model assumes that the surface characteristics are uniform on the side walls and the bottom of each cell. In reality, the samples we tested had unknown emissivity values on the cell bottoms, which were coated with the adhesive used to bond the honeycomb core onto its sink plate. The model showed that for this aspect ratio the emissivity of the hole had a very minor effect on the hole's emissivity.

Test Samples

We tested three different honeycomb configurations, and TABLE 1 lists their specifications. Here the "cell size" is effectively the hexagon diameter. The cells were coated with Chemglaze™ Z307, a robust and relatively high-emissivity paint used in space-flight applications. The average coating thickness was determined by weighing the samples before and after painting. The third sample was made with very thin cell walls and coatings to try for a drastically lower mass per unit area. An unpublished report of an internal NASA study [3] indicated that this paint's emissivity is independent of its thickness over a thickness range of 36 to 117 microns and at temperatures from 30 to 300 Kelvin. Also, a study of Z307 painted on a large chamber wall showed that blackbody radiation below room temperature reflected off it more than 98% specularly [4].

Sample #	Core Thickness	Cell Size	Core Foil Thickness	Avg. Core Coating Thickness
1	12.7 mm	3.175 mm	38.1 μ	16.3 μ
2	9.525 mm	3.175 mm	50.8 μ	17.0 μ
3	9.525 mm	3.175 mm	17.8 μ	8.4 μ

TABLE 1. The specifications of the three tested honeycomb samples

EXPERIMENTAL METHOD

Our approach to measuring the honeycomb's emissivity is a variation on an innovative technique we developed to characterize relatively thin BIRB™ coatings, and it has been described in detail elsewhere [1]. In the earlier measurements we employed a simple geometry, consisting of a thin "sample" disk suspended inside a short, squat "can." The entire assembly fit inside a small cryostat with a 25 cm diameter × 25 cm tall test volume. The disk's top and bottom surfaces and the inside surfaces of the can's "lids" were all prepared with identical BIRB™ coatings. The spacing between the facing coated surfaces was small relative to the diameter, so we approximated a simple textbook case of heat exchange between two infinite parallel surfaces. In the idealized case we would have:

$$\dot{Q} = \frac{\sigma A(T_1^4 - T_2^4)}{\dfrac{1}{\varepsilon_1} + \dfrac{1}{\varepsilon_2} - 1}, \tag{2}$$

with T_1, T_2, ε_1, and ε_2 the warm and cold temperatures and emissivities, respectively [5]. We controlled T_1 and T_2, with small $\Delta T = T_1 - T_2$ values, measured the controlling power of the warm sample, and were able to determine the emissivity ε (T_{avg}). In these earlier measurements the identical coatings on the warm and cold sides provided advantages, leading to extremely precise emissivity measurements of BIRB™.

The honeycomb samples were too thick to configure in this way. If we had bonded honeycomb to the top and bottom of the sample disk, we would have had prohibitively large edge effects on the disk assembly. Instead, we used a hybrid configuration, with the same BIRB™-coated sample disk characterized earlier. Honeycomb core was bonded to the inside of the can's "lids," which were spaced away from the can's center to position the honeycomb inner edges close to the BIRB™ surfaces.

The honeycomb configuration is shown schematically in FIGURE 2. It was only slightly larger than the BIRB™ setup, and it fit into the same small cryostat. The hot "sample" was an aluminum 1100 disk coated on both sides with BIRB. Two tiny thermometers and a heater circuit were imbedded inside it. The sample's outer edge was coated with shiny aluminized tape. It hung midway between two cold plates, each of which had bonded to it honeycomb core facing the sample and a thermometer mounted on its outer side. The cold plates were both bolted to a narrow spacer ring that ran between them near their outer edges. The spacing ring's inner radial surface was polished optically smooth, and a heater wire was wound around and epoxied to its outer edge. The cold plates and spacer ring formed a "can," which completely surrounded the sample. The can sat atop a stainless steel ring that was bolted to the sink plate of a 7 Kelvin cryostat cooled by a Gifford-McMahon cryocooler. A charcoal getter was mounted on the sink plate to adsorb any helium remaining in the system after pump-out. An aluminum cryostat sink shield, bolted to this cryostat plate, encased the entire experiment inside a chamber which ranged from 7 to 30 Kelvin, depending on the experiment temperature.

The BIRB-coated sample's heater and thermometer leads, which supported it mechanically, ran from three holes in its outer edge diagonally outward and upward through slots in the support ring and upper cold plate. These slots did not interfere with the upper cold plate's honeycomb core. The leads ran through drilled threaded rods mounted on an aluminum suspension ring, which was supported above the can on a G-10 ring. The holes in the rods were filled with epoxy, which mechanically and thermally attached the
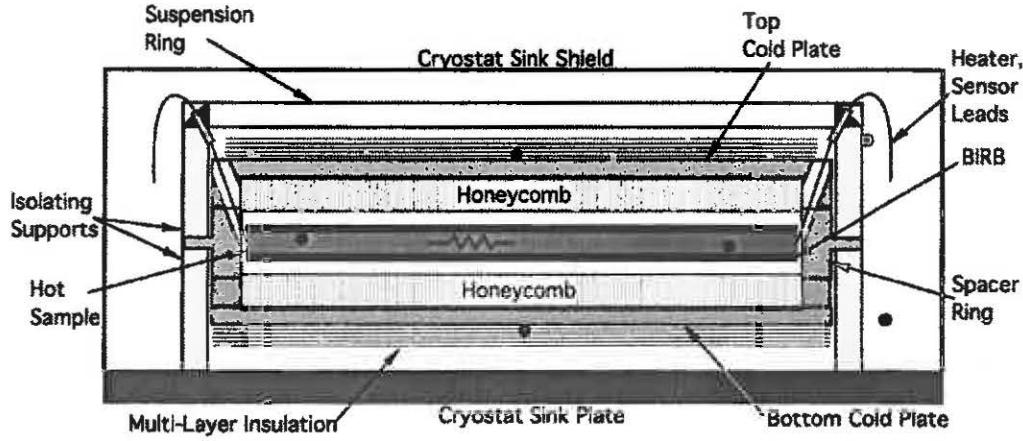
FIGURE 2. A schematic view of the test apparatus. The BIRB is shown as thick black lines on the hot sample, suspended between honeycomb samples bonded to colder plates above and below.

leads to this ring. A thermometer and wire-wound heater were attached to the suspension ring. Multi-layer insulation was installed on the outsides of the cold plates.

As in the earlier BIRB™ measurements we used the fact that:

$$(T_1^4 - T_2^4) \approx 4 \cdot T_{avg}^3 \cdot \Delta T , \qquad (3)$$

with $T_{avg} = (T_1+T_2)/2$. For values of ΔT less than 6% of the average temperature, $T_1^4 - T_2^4$ is linear in ΔT to better than 0.1%. Using this linearization and the fact that we already knew the BIRB emissivity (ε_2), we had:

$$\varepsilon_1 = \cfrac{1}{4\sigma A \overline{T}^3 \left(\cfrac{d\Delta T}{d\dot{Q}} \right) + 1 - \cfrac{1}{\varepsilon_2}} \qquad (4)$$

We measured $\dot{Q}$ vs. ΔT while keeping T_{avg} constant, and the slope of these values in Equation (4) gave us the ε_1 value.

It should be noted that we used the hybrid setup (with BIRB™ on one side and honeycomb on the other) out of necessity, rather than by choice. With identical coatings on the hot and cold surfaces, the dominant uncertainty is in the determination of a single ΔT vs. power slope value. In the hybrid scheme, the uncertainty in the honeycomb emissivity has contributions from both the original BIRB™ measurement and the later slope determination. Obviously we can never have error bars smaller than those on the data we measured in 2011.

Another more subtle issue is the fact that the wavelength spectra of the radiation produced by honeycomb and BIRB™ are not guaranteed to have the same shape at a given temperature. Equation (2) is only strictly true for a given wavelength. However, we assume that most relevant spectra are proportional to the blackbody spectrum, so the total hemispheric emissivities should obey the equation. If the spectra had significantly different shapes, the overall heat exchange might be somewhat different, but this is probably not significant for the very-black coatings we are studying. When the surfaces are identical this issue certainly does not exist.
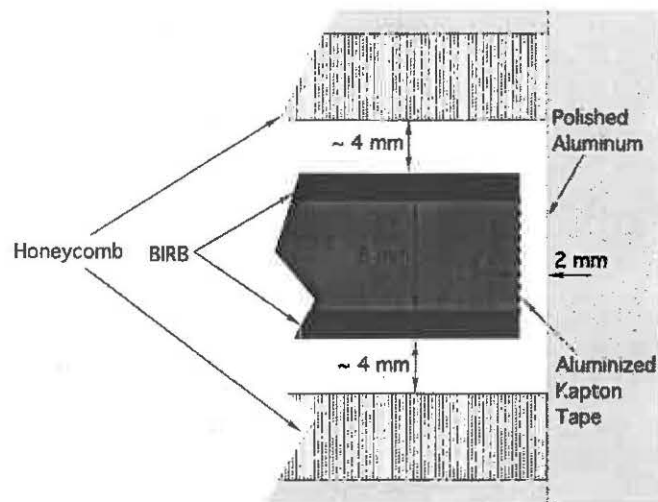
FIGURE 3. A schematic view of edge of the hot sample inside its cold enclosure. The shaded areas are 1100 aluminum. The BIRB thickness is approximate, and assumed here to be 2 mm.
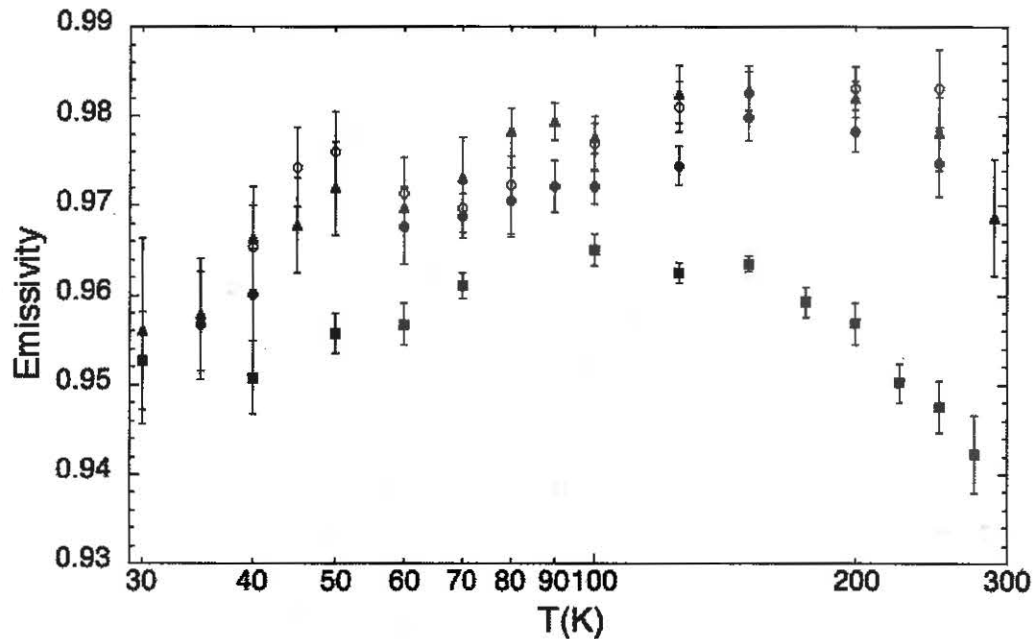
Edge Effect Correction

We built a Thermal Desktop® model of our apparatus to guide the design and to evaluate the validity of the "infinite plane" assumption and Equation 2. The model did not include conduction, but used RadCAD® to compute radiation exchange factors and view factors with a Monte-Carlo ray-tracing algorithm. FIGURE 2 is a schematic view showing the outer edges of the sample and cold plates and the inside of the spacer ring. This geometry was used in the thermal model, although the BIRB™ thickness is an approximation. The error in the infinite plane model is due to the fact that the cold surfaces are slightly larger than the facing ones on the hot sample. As a result, more heat is radiated from cold to hot, and the net heat out of the hot sample is reduced. If this were ignored, the indicated emissivity would be falsely low. It is strictly a geometric effect which can be corrected by using an area, A, in Equation (4) which is about 1% smaller than that of the hot sample. The thermal model shows that using this area in Equation (4) gives the correct surface emissivity.

Data Acquisition and Reduction

The power vs. ΔT measurement technique has been described in detail elsewhere [1]. A LabVIEW™ program controlled the experiment semi-automatically. For each experimental average temperature value, the power was measured at up to ten different temperature gradients. To set up these gradients, the sample and the cold plate temperatures were controlled at values such that the average temperature remained constant. The suspension ring was always controlled at the same temperature as the sample, nearly eliminating any heat conduction in the wires suspending the sample.

For each average temperature, a linear least-squares fit was applied to the steady-state ΔT versus control power. The resulting slope ranged from 11000 K/Watt at 20 K to 4.2 K/Watt at 275 K. It was used in Equation 4 to compute the emissivity. Using only the slope eliminated systematic error due to thermometer calibration offsets, which remained constant over the small range of ΔT values. It also eliminated error due to any constant heat leaks into or out of the sample, such as wire conduction resulting from a constant temperature offset between the sample and suspension ring. The uncertainty in the slope

FIGURE 4. The measured Emissivity vs Temperature. The triangles are Sample 1, open circles are Sample 2, and closed circles are Sample 3. The squares are data for the BIRB™ on the hot sample disk. All these data have been corrected for the edge effect, as described in the text.

was derived using standard linear regression analysis. This uncertainty decreased with increasing number of ΔT values, and our automated system allowed us the luxury of taking enough data to drive each slope error down to an acceptable value.

RESULTS AND ANALYSIS

FIGURE 4 shows the measured emissivity as a function of temperature, including the edge effect correction. Also shown are data from the BIRB™ on the hot sample disk, which was measured back in 2011. The BIRB™ values differ slightly from those published in 2012 because the adjustment for the edge effect was applied incorrectly at that time. As mentioned earlier, the honeycomb error bars represent the uncertainty in ε due to the slope uncertainty and the uncertainty in the BIRB™ emissivity as measured in 2011. Differences among the three honeycomb samples are comparable to the error bars. The fact that all three have emissivities above 0.95 at temperatures down to 30 Kelvin is very good news for JWST.

We used the Goddard Z307 paint emissivity data for thin coatings [3] in our thermal model to predict the temperature dependence of Sample 3's emissivity. FIGURE 5 shows the results for three different assumed specularity values. Curiously, the prediction for 50% specularity is the best match to the data. Since our chamber-wall measurements indicate that thermal radiation reflects totally specularly off Z307 paint, it is not clear why the measured emissivity is not even higher.

CONCLUSION

The results of our emissivity measurements indicate that JWST has flexibility in using painted aluminum honeycomb on some of its radiators. They will likely choose to fly the configuration used in sample 3 and will be able to reduce the system mass. In addition, the relatively small uncertainty in the emissivity will contribute to reducing the overall uncertainty in their thermal model. The fact that the thermal model does not predict
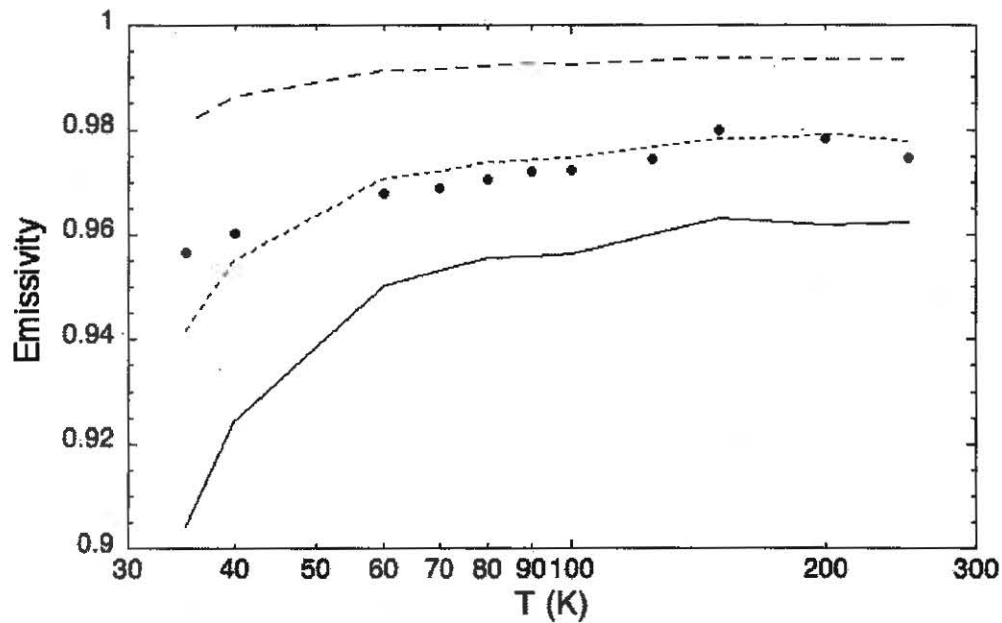
FIGURE 5. The predicted emissivity of Sample 3 for three different specularity values, along with the data. The solid, dotted and dashed lines are 0%, 50%, and 100% specular respectively.

the honeycomb emissivity very accurately makes measurements like these even more valuable.

ACKNOWLEDGEMENTS

REFERENCES

1. Tuttle, J., et al., "A High-Resolution Measurement of the Low-Temperature Emissivity of Ball Infrared Black," in Advances in Cryogenic Engineering 57B, Edited by J. G. Weisend et al., AIP, New York, 2012, pp1505-1512.
2. Sparrow, et al., 1964.
3. Kauder, L., internal NASA memo.
4. DiPirro, M. Tuttle, J., Canavan, E, and Shirron, P., "Use of Cold Radiometers in Several Thermal Vacuum Tests," in Advances in Cryogenic Engineering 57B, Edited by J. G. Weisend et al., AIP, New York, 2012, pp 1513-1518.
5. See, for example, Eckert, E.R.G, and Drake, R.M., Analysis of Heat and Mass Transfer, McGraw-Hill, New York, 1972, p. 632.